J Neurophysiol 106: 127–137, 2011.
First published March 30, 2011; doi:10.1152/jn.01126.2010.

Serotonergic modulation of startle-escape plasticity in an African cichlid fish: a single-cell molecular and physiological analysis of a vital neural circuit

K. W. Whitaker,[1,2]* H. Neumeister,[3]* L. S. Huffman,[4,5] C. E. Kidd,[4] T. Preuss,[3]† and H. A. Hofmann[1,4,5]†

[1]*Institute for Neuroscience, University of Texas at Austin, Austin, Texas;* [2]*Army Research Laboratory, Aberdeen Proving Grounds, Maryland;* [3]*Department of Psychology, CUNY Hunter College, New York, New York; and* [4]*Section of Integrative Biology and* [5]*Institute for Cellular and Molecular Biology, University of Texas at Austin, Austin, Texas*

Submitted 27 December 2010; accepted in final form 24 March 2011

Whitaker KW, Neumeister H, Huffman LS, Kidd CE, Preuss T, Hofmann HA. Serotonergic modulation of startle-escape plasticity in an African cichlid fish: a single-cell molecular and physiological analysis of a vital neural circuit. *J Neurophysiol* 106: 127–137, 2011. First published March 30, 2011; doi:10.1152/jn.01126.2010.—Social life affects brain function at all levels, including gene expression, neurochemical balance, and neural circuits. We have previously shown that in the cichlid fish *Astatotilapia burtoni* brightly colored, socially dominant (DOM) males face a trade-off between reproductive opportunities and increased predation risk. Compared with camouflaged subordinate (SUB) males, DOMs exposed to a loud sound pip display higher startle responsiveness and increased excitability of the Mauthner cell (M-cell) circuit that governs this behavior. Using behavioral tests, intracellular recordings, and single-cell molecular analysis, we show here that serotonin (5-HT) modulates this socially regulated plasticity via the 5-HT receptor subtype 2 (5-HTR_2). Specifically, SUBs display increased sensitivity to pharmacological manipulation of 5-HTR_2 compared with DOMs in both startle-escape behavior and electrophysiological properties of the M-cell. Immunohistochemistry showed serotonergic varicosities around the M-cells, further suggesting that 5-HT impinges directly onto the startle-escape circuitry. To determine whether the effects of 5-HTR_2 are pre- or postsynaptic, and whether other 5-HTR subtypes are involved, we harvested the mRNA from single M-cells via cytoplasmic aspiration and found that 5-HTR subtypes 5A and 6 are expressed in the M-cell. 5-HTR_2, however, was absent, suggesting that it affects M-cell excitability through a presynaptic mechanism. These results are consistent with a role for 5-HT in modulating startle plasticity and increase our understanding of the neural and molecular basis of a trade-off between reproduction and predation.

Mauthner cell; single-cell polymerase chain reaction; *Astatotilapia burtoni*; 5-HT receptor subtype 2; ketanserin

BRAIN AND BEHAVIOR ARE SCULPTED by an intricate and dynamic interplay between genotype, prior experience, and an individual's current social and physiological state (Hofmann 2003; Robinson et al. 2008; O'Connell and Hofmann 2010). Understanding how social life in particular affects brain function at all levels of biological organization is a fundamental question in modern biology (McClung and Nestler 2008). Social experiences manifest themselves as changes in gene expression, neurochemical balance, neural circuit function, and structural reorganization in various brain regions (Edwards and Kravitz 1997; Feder et al. 2009; Fernald 2002; Hofmann 2003). In vertebrates, much of this work has focused on fore- and midbrain circuits, such as the mesolimbic reward system and the social behavior network, because these systems regulate incentive salience and social behavior, respectively (Deco and Rolls 2005; Goodson et al. 2005; Newman 1999; O'Connell and Hofmann 2010, 2011). Also, their function can vary profoundly either as a consequence of social experience or in relation to sex-typical behavior (e.g., Crews 2003; Krishnan and Nestler 2008).

The genetic and physiological analysis of the consequences of social experience at the level of identified neurons has been invaluable (Dickson 2008; Edwards and Kravitz 1997; Yeh et al. 1996). In vertebrates, natural social behavior and the underlying neural substrates are typically not amenable to detailed in vivo neurophysiological studies. Thus, to reveal the neural mechanisms that link molecular and endocrine processes to social life, it is essential to study distinct and robust behavior patterns associated with the overall phenotypic state of an individual. Invertebrates have proven to be excellent model systems for such an integrative approach (Edwards and Kravitz 1997). In crayfish, for example, social control of escape behavior and subsequent modification of the underlying neural circuitry (such as the lateral giant neuron system) through serotonergic pathways has provided a powerful conceptual framework and important insights into the neurophysiological effects of social experience (Antonsen and Edwards 2007; Edwards et al. 1999, 2003; Spitzer et al. 2005; Yeh et al. 1996, 1997). However, few, if any, vertebrate model systems lend themselves to such an approach.

The African cichlid fish *Astatotilapia burtoni* has become an important model system in social neuroscience (Hofmann 2003; Robinson et al. 2008; Wong and Hofmann 2010). Males of this species display remarkable behavioral and neural plasticity throughout life (Hofmann 2003; Robinson et al. 2008; Wong and Hofmann 2010), as they repeatedly change status in a social dominance hierarchy (Hofmann and Fernald 2000). When an individual is dominant (DOM) in a social group, he maintains bright body coloration and displays a diverse behavioral repertoire to defend a territory and attract females for mating. In contrast, subordinate males (SUBs) display few distinct behavior patterns, adopt cryptic coloration, and school with conspecifics. These traits make individual SUBs difficult to distinguish from the school (Turner and Pitcher 1986) and from the surrounding environment but severely limit their reproductive opportunities (Fernald and Hirata 1977). Since

* K. W. Whitaker and H. Neumeister contributed equally to this work.
† T. Preuss and H. A. Hofmann contributed equally to this work.
Address for reprint requests and other correspondence: H. A. Hofmann, Univ. of Texas at Austin, Section of Integrative Biology, 1 University Station—C0930, Austin, TX 78712 (e-mail: hans@mail.utexas.edu).

DOMs are more conspicuously colored and isolated from the school, they are likely more vulnerable to predation than SUBs (Fernald and Hirata 1977; Maan et al. 2008). We have previously shown (Neumeister et al. 2010) that the trade-off between reproductive opportunities and predation risk leads to a robust difference between DOMs and SUBs in startle-escape performance: behavioral responses to sound clicks of various intensities revealed significantly higher startle-escape responsiveness in DOMs compared with SUBs.

This behavioral plasticity can be explained at least in part by social status-dependent variation in the excitability of the Mauthner cells (M-cells) that triggers the startle-escape behavior (Neumeister et al. 2010). The M-cell is a sensory integrator that initiates an escape response in most teleost fishes and larval amphibians and constitutes a powerful model system for deciphering the cellular mechanisms underlying simple decision-making processes in the nervous system (Preuss et al. 2006; Schlegel and Schuster 2008; for review see Korn and Faber 2005). Moreover, M-cell activity and membrane properties directly control the expression of the behavior (Neumeister et al. 2008; Preuss and Faber 2003; Weiss et al. 2006). M-cell responses to auditory stimuli have been studied in detail even though this circuit can also be activated by visual and lateral line inputs (Canfield 2003; Canfield and Rose 1996; Preuss et al. 2006). In the case of 8th nerve afferents, some axons form mixed electrical-chemical synapses onto the distal portion of each M-cell's laterally projecting dendrite (Kohno and Noguchi 1986; Pereda et al. 2003) and onto inhibitory interneurons [so-called passive hyperpolarizing potential (PHP) cells], which in turn synapse onto the M-cell soma and dendrites (Furukawa and Furshpan 1963; Satou et al. 2009; Weiss et al. 2008). M-cell axons decussate and form en passant synapses with recurrent and contralateral inhibitory interneurons as well as motoneurons along the contralateral body wall (Faber and Korn 1978). Thus a loud, unexpected sound may trigger a contraction along one body wall of the fish, pulling the head and tail together into a "C" shape ("phase 1" of the startle-escape response according to Eaton et al. 1991) with a latency as short as 8 ms.

Previous studies have shown adaptive changes in M-cell excitability in response to altered environmental conditions (Preuss and Faber 2003; Szabo et al. 2008) and during sensory gating (Neumeister et al. 2008). In addition, we recently demonstrated (Neumeister et al. 2010) that in *A. burtoni* M-cells of DOMs exhibit larger excitatory responses to sound clicks in a manner consistent with the increase in behavioral responses. We also found that the inhibitory drive mediated by PHP cells presynaptic to the M-cell is significantly reduced in DOMs. This study showed for the first time that escape probability can vary with social status, and that these differences are due to changes in M-cell excitability. More generally, these insights provided an integrative explanation of an ecological and social trade-off at the level of an identifiable decision-making circuit. The neurochemical basis of this plasticity, however, remains to be determined.

The biogenic amine serotonin (5-hydroxytryptamine, 5-HT) is a prominent neuromodulator of social behavior (Edwards and Kravitz 1997; Veenema 2009). In crustaceans, higher 5-HT levels are typically associated with increased aggression and social dominance (Edwards and Kravitz 1997). Moreover, in crayfish 5-HT has been shown to modulate the lateral giant escape reflex differentially in DOMs and SUBs, facilitating and inhibiting, respectively (Krasne et al. 1997; Yeh et al. 1997). These studies also suggested that differential expression of 5-HT receptors (5-HTRs) is controlled by social status (Edwards et al. 2002). In vertebrates, however, higher levels of 5-HT are generally believed to lower aggression. Importantly, Winberg et al. (1997) found that in the brain stem of *A. burtoni* males 5-HT metabolism is higher in SUBs compared with DOMs. Also, intracranially administered 5-HT inhibits aggressive behavior in the Blue Acara cichlid, *Aequidens pulcher* (Munro 1986). Several physiological and morphological studies have suggested that 5-HT modulates the M-cell system. Local 5-HT administration enhances tonic and evoked inhibitory currents observed in the M-cell (Mintz et al. 1989; Mintz and Korn 1991). Moreover, immunohistochemical studies in goldfish and zebrafish (Gotow et al. 1990; McLean and Fetcho 2004; Petrov et al. 1991) demonstrated at least two types of serotonergic inputs onto the soma and dendrites of the M-cell, underscoring the putative role of this neuromodulator for this system.

Despite extensive pharmacological studies examining M-cell neurotransmitter systems (see above), very little work has focused on the molecular level. The only exception has been the study by Imboden et al. (2001), who cloned and sequenced three glycine receptor subunits from zebrafish and provided evidence that glycine is a major inhibitory neurotransmitter acting on the M-cells. Despite the important neuromodulatory role 5-HT plays in M-cell function, there have been no molecular studies.

In the present study, we pharmacologically perturbed the function of the 5-HTR subtype 2 (5-HTR_2) in *A. burtoni* DOMs and SUBs and showed that 5-HT plays an important role in determining the socially regulated plasticity in startle-escape performance we have described previously for this species (Neumeister et al. 2010). Using transcriptomics, we then demonstrated that high-quality mRNA can be harvested from single M-cells, paving the way for single-neuron molecular analyses of the M-cell system. Finally, we showed that only a subset of 5-HTR subtypes is expressed in the M-cell. Together, these results provide a compelling foundation for the integrative analysis of a socially regulated neural circuit in a highly social vertebrate.

MATERIALS AND METHODS

Animals. Adult *A. burtoni* from a lab-reared stock were housed in acrylic tanks (30 × 30 × 60 cm) in communities of 8–12 males and 8–12 females under conditions mimicking the natural environment in their native Lake Tanganyika (pH 8.5 ± 0.2; 27 ± 0.2°C; 12:12-h light-dark cycle). Gravel substrate and terracotta pots were provided to allow multiple males to establish territories within each community. For the individuals used in this study, we assessed dominance status at least twice weekly for more than 2 wk to identify stable DOMs and SUBs, using established methods (Renn et al. 2008). All experimental protocols were reviewed and approved by the Institutional Animal Care and Use Committees of Hunter College of CUNY and the University of Texas at Austin.

Assessing startle behavior. To evaluate auditory startle responses in male *A. burtoni* we used a paradigm identical to the one described by Neumeister et al. (2010). Briefly, isolated fish were transferred to a restricted arena (~17 cm in diameter, 22 cm deep) within a larger (110 liter) tank between two underwater speakers (UW30, Electro Voice, Burnsville, MN) and filmed from above with a high-speed camera (resolution 512 × 384 pixels, 1,000 frames/s; Kodak Extapro

1000 HRC, Eastman Kodak, San Diego, CA). Three stimulus intensities (155, 157, and 160 dB) were presented in randomized order within each of four blocks of stimuli with variable intertrial intervals (range: 2–10 min). To account for variation in stimulus intensity as a function of distance from the loudspeaker and other factors, we systematically measured stimulus intensities (at given loudspeaker settings) throughout the test arena. This information enabled us to present a defined stimulus intensity to a fish independent of its respective location. Fish were allowed to acclimate for 50 min before the first 200-Hz sound stimulus was presented. Individual startle probabilities were calculated from the number of C-starts occurring within a given number of trials compared with the total number of trials.

M-cell electrophysiology. The electrophysiological experiments involved the same surgical, stimulation, and recording techniques as described by Neumeister et al. (2010). Fish were initially anesthetized for 3–5 min by bath immersion in MS-222 (120 mg/l), fixed in the recording chamber with two pins, and respirated through the mouth with a steady flow of aerated saline containing the general anesthetic MS-222 at a concentration of 20 mg/l. Before dissection, a topical anesthetic (20% benzocaine gel, Ultradent) was applied to the incision sites and fish were immobilized with intramuscular injections of *d*-tubocurarine (1–3 μg/g body wt). A small hole in the cranium exposed the medulla for somatic M-cell recordings. A small lateral incision at the caudal midbody exposed the spinal cord to bipolar electrodes for antidromic activation of the M-axons with small pulses (5–8 V) with an isolated stimulator. Antidromic stimulation produces a negative potential in the M-cell axon cap (typically >15 mV), which unambiguously identifies its axon hillock and allows intracellular recordings from the M-cell soma or along the lateral dendrite at defined distances from the axon hillock (Faber and Korn 1978).

Postsynaptic responses (PSPs) to sound stimuli before and after drug application (see below) were recorded in the M-cell with sharp glass electrodes (10–12 MΩ) filled with 5 M potassium acetate (CH_3CO_2K) with an Axoprobe-1A amplifier in current-clamp mode. Sound stimuli consisted of 200-Hz sound pips produced by a subwoofer with underwater intensities ranging from 126 to 133 dB re. 1 μPa in water. Auditory stimuli were recorded with a microphone positioned above the fish during the experiments and with a hydrophone (SQ01; Sensor Technology, Collingwood, ON, Canada) inside the recording chamber tank for stimulus calibration trials. Throughout the experiments (typically 2–3 h), we monitored the M-cell resting membrane potential (RMP). Cells with an RMP less negative than −76 mV and experiments with >10% changes in RMP were excluded. Experimental constraints (see Neumeister et al. 2010 for details) limited the achievable maximal underwater sound intensity in the recording chamber to 133 dB re. 1 μPa in water (which corresponds to ~60 dB SPL in air re. 20 μPa).

Statistical analysis. Receptor antagonist-evoked changes in PSP amplitude in SUBs and DOMs were analyzed with a repeated-measures ANOVA in JMP 8 (Statistical Discovery Software, SAS Institute, Cary, NC). Subsequently, we used a generalized linear mixed model (GLMM) analysis to assess differences between the three stimulus intensities, with subject identity included as a random effect. A post hoc Student's *t*-test was applied to the least squares means of the evoked PSP responses for the three stimulus intensities.

5-HTR$_2$ pharmacology. The selective 5-HTR$_2$ antagonist ketanserin (S006, Sigma) was used in behavior and electrophysiological experiments. Although a large number of pharmaceutical agents have known efficacy for mammalian serotonin receptor subtypes, only ketanserin has been examined in teleosts (*Brachyhypopomus pinnicaudatus*: Allee et al. 2008; *Danio rerio*: Brustein et al. 2003). To test the role of 5-HTR$_2$ in freely behaving males of different social status, ketanserin was used similar to the study of Allee et al. (2008). Briefly, the drug was dissolved in physiological saline (in mmol/l: 114 NaCl, 2 KCl, 4 $CaCl_2 \cdot 2H_2O$, 2 $MgCl_2 \cdot 6H_2O$, 2 HEPES) and 5% ethanol, and pH was adjusted to 7.2 with NaOH. DOM (n = 8) and SUB (n = 8) males were injected intraperitoneally (IP) with 10 μg/g body mass of the drug in volumes of 50–150 μl. This concentration was selected based on a preliminary dose-response experiment and did not result in any nonspecific effects on behavior. Experimental trials began 10 min after injection and lasted as long as 70 min after injection. The same concentration of ketanserin was injected intramuscularly (IM) during the electrophysiological experiments, dissolved either in the saline-ethanol vehicle described above (n = 5) or in 20% DMSO (n = 3). We then examined electrophysiological M-cell properties of four DOMs and four SUBs within 0.5–2 h of drug exposure. No differences were observed in relation to the vehicle used. It should be noted that different routes of administration (e.g., slow vs. fast) might alter the effect of the drug on neuronal functioning (Teshiba et al. 2001), although it seems unlikely that the rate of bioavailability would differ significantly between IM and IP injections (as opposed to, e.g., intracerebroventricular vs. oral administration). In addition, because only a single dose was applied by IM/IP administration, ketanserin likely reached the brain in a single bolus as opposed to multiple peaks.

Immunohistochemistry. We used immunohistochemistry to visualize 5-HT in the *A. burtoni* hindbrain according to the procedure described by Gotow et al. (1990). Fish were euthanized under anesthesia (200 mg/l MS-222 for 10 min), and the brain was quickly removed and placed into freshly prepared 4% paraformaldehyde in 0.1 M phosphate buffer (pH 7.5) at 4°C overnight. After rinsing with 0.1 M phosphate buffer the brain was cryoprotected in 30% sucrose at 4°C overnight and embedded in OCT compound (Sakura Finetek, Torrance, CA). We then prepared 30-μm transverse sections of the embedded brain stem on a cryostat. Sections were transferred onto precoated Superfrost Plus slides (Fisher Scientific, Pittsburgh, PA; Erie Scientific, Portsmouth, NH), air-dried, rehydrated with 0.1 M phosphate buffer, quenched with 1% hydrogen peroxide (H1009, Sigma-Aldrich) for 10 min, and rinsed again. Nonspecific binding sites were blocked with 1% bovine serum albumin (A7906, Sigma-Aldrich), 1.5% heat-inactivated normal goat serum (Vector Laboratories, Burlingame, CA), and 0.02% saponin (S7900, Sigma-Aldrich) for 1 h at room temperature. After rinsing, slides were incubated overnight with primary rabbit anti-5-HT polyclonal antibody (1:2,000; Sigma S5545). After several rinses, they were then incubated with goat anti-rabbit IgG secondary antibody (1:200) for 1 h at room temperature. Immunolabeling was assessed by adding drops of avidin-biotin-peroxidase complex (Vectastain ABC peroxidase kit, Vector Laboratories) onto each slide. After rinsing, diaminobenzidine tetrahydrochloride (DAB; Vector Laboratories) solution was applied for visualization. Rinsed sections were then air-dried overnight and dehydrated through an alcohol series (2 × 70%, 2 × 95%, 2 × 100%). Slides were counterstained with cresyl violet. Finally, slides were mounted with Permount (SP15, Fisher Scientific) and viewed with an Aristoplan microscope (Leitz). To confirm that background staining did not affect our interpretation of the signal, we conducted controls without primary antibody. Several brains were only stained with cresyl violet for morphological analysis.

RNA isolation, amplification, and quality control. RNA was isolated from whole brain of three *A. burtoni* individuals (1 DOM, 1 SUB, 1 female) and from single M-cells of three fish. For the whole brain sample, the tissue was homogenized in 500 μl of TRIzol (Invitrogen) and processed according to the manufacturer's instructions. Pellets were redissolved in RNA Storage Solution (Ambion). For single-cell RNA isolation, we harvested the cytoplasm of one M-cell each from one DOM, one SUB, and one female at the end of the respective electrophysiological recording session. We aspirated the cytoplasm with a low-resistance (2–4 MΩ) glass electrode pulled from 3-mm glass with a vertical puller (PE-22, Narishige) filled with a 2.5 M KCl solution made up with RNase-free water. After penetration of the M-cell, we applied a small negative pressure for ~15–20 min with a 60-ml syringe and aspirated the cytoplasmic contents into the tip of the electrode. During aspiration we monitored the M-cell RMP and, every 4 s, the amplitude of an antidromically evoked M-cell spike (i.e., input resistance) to verify a good seal. The electrode was

then quickly removed, the tip broken off, immediately frozen in powdered dry ice, and stored at −80°C until RNA isolation and amplification. To avoid contamination from extracellular sources, the electrodes were coated before the experiment with a film of Sigmacote (Sigma; neutral, hydrophobic film on the electrode surface), which repels water, retards clotting, and prevents adsorption of macromolecules. We extracted the RNA by previously established protocols (Baugh et al. 2001; Duftner et al. 2008).

We subjected the RNA samples obtained from the three whole brains and the three M-cells (2 replicates each) to two rounds of linear amplification. Linear RNA amplification strategies based on in vitro transcription with T7 RNA-polymerase are generally prone to lose sequence information at the 5′ end. This is mainly due to *1*) the alignment of the T7-promoter/oligo(dT) primer and the transcription start at the 3′ poly(A)-tail of the original mRNA and *2*) the use of random hexamers during the second cDNA synthesis step, causing reduction of fragment length. To facilitate the generation of almost full-length molecules we used the picoRNA amplification system by Ocimum Biosolutions, which is based on Baugh et al. (2001) with the following modifications. For first-round amplification, in place of the First Strand cDNA Synthesis Mix 1, was 0.75 μl of 10× Primer A, 0.5 μl of dNTPs, and 0.75 μl of DEPC H_2O. In place of First Strand cDNA Synthesis Mix 2 was 2 μl of 5× RT Buffer, 0.5 μl of RNAase Inhibitor, 0.5 μl of RT Enzyme, and 3 μl of DEPC H_2O. In place of RNAase Mix 3 was 0.5 μl of RNAase. In place of Second Strand cDNA Synthesis Mix 4 was 0.5 μl of 10× Primer B, 0.5 μl of dNTPs, 3 μl 5× Extender Buffer, and 10 μl of DEPC H_2O. In place of Extender Enzyme A Mix 5 was 0.5 μl of Extender Enzyme A. In place of Primer Erase Mix 6 was 0.5 μl of Primer Erase. In place of Primer C was 1.0 μl of 10× Primer C. In place of Extender Enzyme B Mix 7 was 0.5 μl of Extender Enzyme B. Yields of amplified RNA were between 37 and 47 μg per sample as measured by spectrophotometry (NanoDrop ND-1000). Assuming that 1–5% of total RNA correspond to poly(A)+ RNA, and the first round of amplification yielded an ~1,000- to 4,000-fold increase while the second round yielded an ~200-fold increase of poly (A)+ equivalents (based on the values provided by the manufacturer of the amplification kit), we estimate that each harvested M-cell contained ~10–30 pg of total RNA.

We have previously shown that the vast majority of RNA species amplify faithfully (Duftner et al. 2008). However, it was not clear to what extent the cytoplasmic aspiration might compromise RNA quality. We therefore determined quality and size distribution of amplified RNA and absence of genomic DNA on a BioAnalyzer 2100 (Agilent) with the Agilent Total RNA NanoChip assay. RNA fragments peaked at ~500 bp and ranged up to 2,000 bp, indicating excellent preservation of even long RNA species.

Transcriptome analysis of M-cells. To assess the amount of variation in M-cell gene expression on a genomic scale, we compared the transcriptomes of the three M-cells to three whole brain samples (where experimental variation can be expected to be minimal). The six RNA samples to be analyzed were paired in a simple loop design (Churchill 2002) such that each sample was directly compared with two samples of the other group (M-cell or whole brain), resulting in six microarray hybridizations. Two technical replicates per sample allowed us to label each sample with both Cy3 and Cy5 dye to control for dye bias. The samples were competitively hybridized to a 19K *A. burtoni* microarray (GEO platform GPL6416) constructed from a brain-specific library and a mixed tissue library representing a total of ~14,660 potential genes (Renn et al. 2004; Salzburger et al. 2008). Protocols for cDNA preparation and hybridization were according to Duftner et al. (2008) with several notable changes: a Qiagen MinElute PCR Purification Kit was used for both cDNA purifications; 1 μl of 5 μg/μl yeast tRNA (Invitrogen) was included in the probe labeling reactions. Hybridization was performed under a coverslip submerged in a humidified chamber (Telechem) at 65°C for 15–16 h in the dark. Slides were rinsed at room temperature, first in 0.6× SSC, 0.025% SDS, 0.001 M DTT and then in 0.05× SSC, 0.001 M DTT, before they were centrifuged until dry. The slides were kept in the dark until they were scanned with an Axon 4000B scanner (Molecular Devices) with the software package Genepix 6.0 (Molecular Devices).

The data were prepared for analysis in a manner similar to that of Renn et al. (2008) with an additional normalization ("within-array batch normalization") to correct for the presence of two different cDNA libraries on our array (Duftner et al. 2008). The normalized intensities were used to calculate ratios of Cy3 to Cy5 intensity for each feature for each array. All raw and processed data are available at the GEO database (www.ncbi.nlm.nih.gov/projects/geo/) under accession number GSE26277.

Between-group (M-cell vs. whole brain) analyses were performed by computing a *t*-statistic for each feature with the LIMMA package (Smyth et al. 2004; Smyth 2005) in R/Bioconductor. We also did an individual analysis using LIMMA in which we made all possible pairwise comparisons between our six samples and corrected for multiple hypotheses testing according to Benjamini and Hochberg's (2000) false discovery rate (FDR) correction method. This analysis necessitates that one sample be designated as a reference, which we arbitrarily chose as M-cell 1.

Sequencing and classification of 5-HT receptor subtypes. To determine 5-HTR expression in single M-cells, we obtained sequences for multiple *A. burtoni* 5-HTRs by a PCR-based approach. The PCR fragments obtained for all receptor subtypes were sequenced. Products similar to 5-HTRs in GenBank were cloned into pCRII-TOPO vectors (Invitrogen). The 5A (CN469330) and 6 (CN469225) subtypes had previously been obtained in *A. burtoni* by expressed sequence tag (EST) analysis (Renn et al. 2004; Salzburger et al. 2008). For the 1A and 1D subtypes, we designed primers based on the orthologous genes in the closely related Nile tilapia, *Oreochromis mossambicus* (GenBank accession nos. AY219038 and AY219039, respectively). To obtain the *A. burtoni* 2A sequence, we designed degenerate primers with CODEHOP (http://blocks.fhcrc.org/codehop.html) based on homologous sequences from stickleback, medaka, and pufferfish obtained by blasting the zebrafish sequence against the genomes of these three species (http://genome.ucsc.edu/). Finally, we obtained the *A. burtoni* 3B sequence by designing degenerate primers with CODEHOP based on the *Carassius auratus* sequence (EF490968.1) and orthologous sequences from stickleback, medaka, and pufferfish again obtained by blasting the zebrafish sequence against the genomes of these three species (http://genome.ucsc.edu/). Table 1 contains information on fragment lengths, number of amplification rounds, and accession numbers, as well as sequence information for the gene-specific primers we designed for subsequent PCR analysis.

Table 1. *Primers used for determining Astatotilapia burtoni 5-HTR sequences*

5-HTR Subtype	Accession No.	Forward Sequence (5′ to 3′)	Reverse Sequence (5′ to 3′)	Product Size, bp
1A	GQ2218441	AAACTTCTCCAGTGGCATCG	GTCTCCAGATCAGCCCTCAG	1,362
1D	GQ227406	CAAAACCATCAGTGCCACAC	CTGCTTGAATTCGTCGTTGA	1,242
2A	GQ227409	GACATGCTGCTGGGCTTC	CACCATGATGGTCAGGGG	393
3A	GQ227408	ATGGACGGATGAGTTCCTTG	GCCATGCAGACCACAAAGTA	675
5A	GQ227407	AGCAGCAAAGTGAAATACGATG	GCCCCAGTTTCCACAGTCT	450
6	GQ227403	CTGGCTCAAACTGCTTCCTG	AGCACAGATGCCACCAGAG	502

5-HTR, serotonin receptor.

On the basis of the partial mRNA sequences obtained, we determined the respective *A. burtoni* amino acid sequences. To assess whether our putative 5-HTR sequences indeed encode the expected subtypes, we used the Mega 4 freeware package (http://www.megasoftware.net/m_con_select.html) to align the sequences with ClustalW to the orthologous protein sequences of multiple species (*Gasterosteus aculeatus*, *Homo sapiens*, *Mus musculus*, *Oryzias latipes*, *Rattus norvegicus*, *Takifugu rubripes*, *Tetraodon nigroviridis*; see Supplemental Table S1 for sequence information) and generate a bootstrapped nearest neighbor-joining gene tree.[1]

Analysis of 5-HT receptor expression in single M-cells. No 5-HTR sequences are present on the microarray (Renn et al. 2004; Salzburger et al. 2008). To determine which, if any, 5-HTR subtypes are expressed in M-cells we used the amplified RNA samples as templates for PCR assays using the gene-specific primers listed in Table 1. cDNAs of subtypes 5 and 6 were denatured for 5 min at 95°C and then amplified over 35 cycles of 95°C for 45 s, 53.3°C for 20 s, 72°C for 60 s with a final elongation at 72°C for 5 min. For subtypes 1A and 1D, there was one round of amplification, then the same process as above. For the 3B subtype, the template was denatured at 94°C for 6 min and then amplified over 40 cycles of 95°C for 45 s, 52.4°C for 30 s, 72°C for 60 s, and a final elongation of 72°C for 10 min. The PCR conditions for 5-HTR_{2A} comprised a 6-min denaturation step at 95°C, 40 cycles of 95°C for 45 s, 54.6°C for 30 s, 72°C for 60 s, and a final elongation at 72°C for 5 min.

RESULTS

Antagonizing 5-HTR_2: startle probability. The presence of ketanserin, a 5-HTR_2 antagonist, significantly increased (ANOVA, $P = 0.0002$) the responsiveness of DOMs (saline: 39.6 ± 7.2%; ketanserin: 70.8 ± 6.9%) and SUBs (saline: 43.8 ± 10.4%; ketanserin: 79.1 ± 8.5%) to short sound pips (Fig. 1). We observed an injection effect that reduced the responsiveness of DOMs and eliminated the difference between males of different status observed in noninjection studies of behavior (Neumeister et al. 2010).

Antagonizing the 5-HT 2A receptor increases M-cell excitability in SUBs. To determine whether 5-HT modulates M-cell excitability via the 2A subtype (5-HTR_{2A}), we quantified in SUBs ($n = 4$) and DOMs ($n = 4$) the effect of the 5-HTR_{2A} antagonist ketanserin on sound-evoked M-cell excitatory postsynaptic potentials (EPSPs) in response to sound pips of various intensities (126, 130, and 133 dB re. 1 μPa in water). After measuring baseline values, we administered ketanserin and analyzed its effect on the M-cell within 0.5–2 h.

Ketanserin evoked differential changes in the postsynaptic (PSP) amplitude in SUBs and DOMs ($F = 25.80$; $P = 0.0023$; repeated-measures ANOVA). In all SUBs tested, ketanserin increased the synaptic response to sound pips as indicated by an overall increase of the somatically recorded PSP (Fig. 2*A*). Interestingly, the observed relative increase in peak amplitude was inversely correlated to sound intensity (Fig. 2*B*, open bars; $P = 0.041$, GLMM). In contrast, the synaptic response in DOMs remained essentially unchanged after application of ketanserin (Fig. 2*B*, filled bars; $P = 0.296$, GLMM).

Consistent with the PSP effects, we also observed differential effects of ketanserin on the M-cell input resistance following activation of the collateral feedback network of inhibitory interneurons in SUBs and DOMs. As discussed previously (Faber and Korn 1978; Neumeister et al. 2010), this powerful

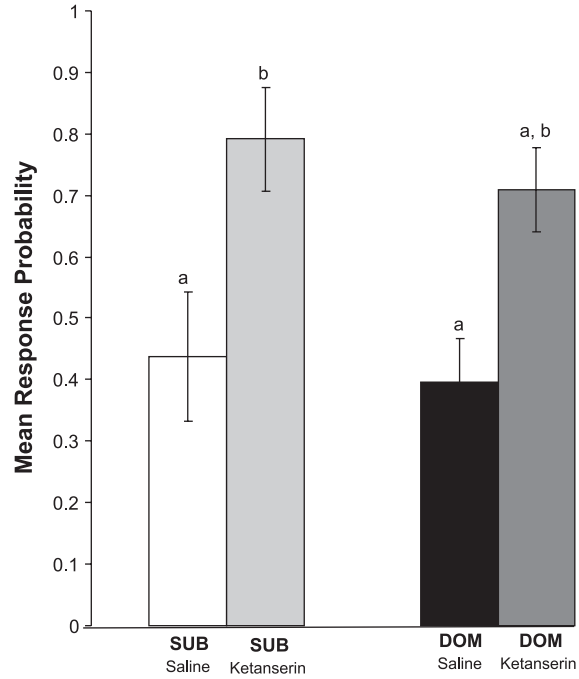

Fig. 1. Startle probability significantly increases in the presence of the serotonin receptor (5-$HTR)_{2A}$ antagonist ketanserin (ANOVA: $P = 0.0002$). We observed an injection effect that reduced dominant male (DOM) responsiveness to the level of subordinate males (SUBs). When treated with ketanserin, however, response probability increased in both DOMs and SUBs. Letters denote homogeneous subgroups, as determined by post hoc testing, such that groups that differ significantly ($P < 0.05$) from each other have different letters.

inhibition is mediated by a Cl^--dependent change in membrane conductance, which effectively shunts incoming excitatory synaptic currents out of the cell. This inhibition can be quantified as the fractional reduction in peak amplitude (inhibitory shunt) of an evoked test action potential (AP) after activating the feedback inhibitory network with a preceding AP. Systematically changing the interstimulus interval (ISI) between the conditioning AP and the test AP exposes the evoked inhibitory time course. This approach is possible because the M-cell's soma and dendrites are unexcitable. An increase in the fractional shunt [defined as $100 - (AP_{test}/AP_{control} \times 100)$] thus indicates a decrease in input resistance.

Specifically, in SUBs ketanserin significantly ($P = 0.03$, paired *t*-test) attenuated the magnitude of inhibition at onset by 28% [mean inhibitory onset shunt: 60.2% ± 1.17 (SE) and 43.16 ± 1.17 (SE) for control and drug, respectively], but inhibition increased in the presence of ketanserin during the later portion of the response (Fig. 2*C*). In contrast, DOMs do not show the initial reduction in inhibition [$P = 0.80$; paired *t*-test; mean inhibitory onset shunt: 48.31% ± 5.91 (SE) and 47.06 ± 1.93 (SE) for control and drug, respectively], yet they exhibit the later (<10 ms) enhancement seen in SUBs (Fig. 2*D*). Indeed, under control conditions inhibition in SUBs is ~20% larger compared with DOMs (black traces in Fig. 2, *C* and *D*). This difference is essentially eliminated by ketanserin (compare gray trace in Fig. 2*C* with black trace in Fig. 2*D*). Thus, as seen with the inhibitory responses, the 5-HTR_2 antagonist ketanserin seems to affect SUBs more than DOMs.

5-HT varicosities envelop M-cell soma and dendrites. Figure 3, *A* and *B*, show the morphology of the paired M-cell in *A. burtoni*. They are located in the anterior part of the hindbrain

[1] Supplemental Material for this article is available online at the Journal website.

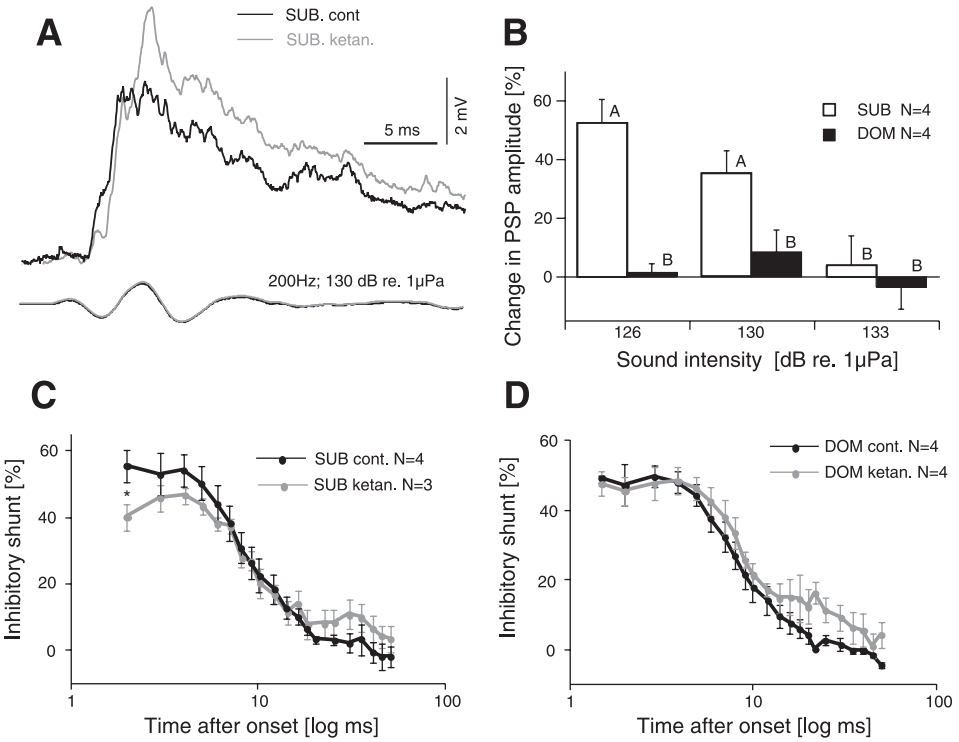

Fig. 2. Differential effects of ketanserin on M-cell properties in SUBs and DOMs. *A*: somatically recorded postsynaptic response (PSPs, averages of 5 sweeps) in a SUB in response to a sound pip before (black) and after (gray) the administration of the 5-HTR_{2A} antagonist ketanserin. *Bottom* trace shows a record of the sound stimulations. *B*: quantification of the effects of ketanserin on the PSP peak amplitude in SUBs and DOMs (means ± SE). The histogram shows the changes in PSP amplitude in response to different stimulus intensities relative to controls after application of ketanserin. Letters indicate homogeneous subgroups such that groups that are significantly ($P < 0.05$) different from each other according to post hoc *t*-tests in a generalized linear mixed model (GLMM) analysis have different letters. *C*: feedback inhibition in SUBs before (black) and after (gray) the administration of ketanserin. Inhibition was quantified in the M-cell soma as the fractional reduction (shunt) of an antidromically evoked test action potential (AP) that followed a conditioning AP. The graph shows the time course and magnitude (means ± SE; $*P = 0.03$) of the inhibitory shunt after test AP onset. *D*: feedback inhibition in DOMs before (black) and after (gray) ketanserin administration; details as in *B* (means ± SE; $n = 4$).

beneath the fourth ventricle, ~700 μm below the surface of the medulla and 150–200 μm lateral from the midline. The M-cell is characterized by a large soma and two major dendrites that extend up to 600 μm dorsolaterally (lateral dendrite, LD) and ventrorostrally (ventral dendrite, VD). The axon hillock is surrounded by the so-called "axon cap" (Fig. 3*C*), a region densely packed with glia cells and nerve fibers that creates a perimeter of high electrical resistance.

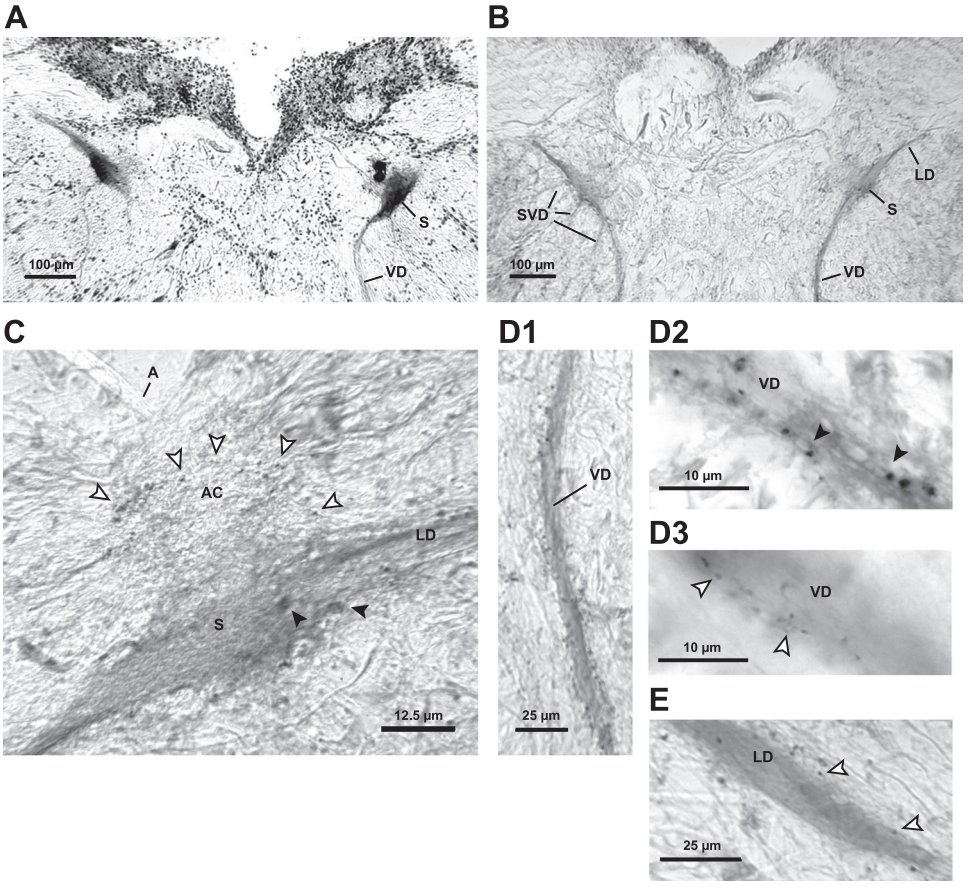

Fig. 3. Morphology and 5-HT immunohistochemistry of the M-cell in DOMs. *A*: cresyl violet stain of both M-cells. *B*: overview of 5-HT immunolabeling of both M-cells. *C*: labeled 5-HT-containing type I and type II fiber varicosities at the soma and axon cap, respectively. The M-cell axon is also visible in this micrograph. *D*: 5-HT labeling at the M-cell ventral dendrite. *D1*: overview showing distribution of 5-HT labeling along the dendrite. *D2* and *D3*: detailed view of type I fibers characterized by larger terminals, or boutons (>1-μm diameter; black arrowheads, *D2*) and of type II fibers characterized by smaller beaded varicosities (<1-μm diameter; white arrowheads, *D3*). *E*: overview showing few beaded varicosities (type II; white arrowheads) at the lateral dendrite. A, axon; AC, axon cap; LD, lateral dendrite; S, soma; VD, ventral dendrite; SVD, small ventral dendrite.

Table 2. *Variation in expression profiles*

	M-Cell 1	M-Cell 2	M-Cell 3		WB 1	WB 2	WB 3
M-cell 1		0.88	0.91	WB 1		0.84	0.86
M-cell 2			0.90	WB 2			0.86
M-cell 3				WB 3			

Pearson correlation coefficients are shown for pairwise comparisons between M-cell (*left*) and whole brain (WB; *right*) transcriptomes.

The latter provides the structural basis for electrical field (ephaptic) inhibition and classical chemical inhibition at the M-cell axon hillock (Bierman et al. 2009; Faber and Korn 1978; Weiss et al. 2008) The axon extends further medially to cross the midline before joining the spinal cord running posterior (Fig. 3*C*).

We used immunohistochemistry to label 5-HT in the *A. burtoni* hindbrain in three animals. As can be seen in Fig. 3, *B–E*, 5-HT-containing profiles are present at the M-cell soma and along the LDs and VDs, with the latter being labeled predominantly (compare Fig. 3, *E* and *D1*, respectively). Similar to the situation in goldfish (Gotow et al. 1990), type I and type II fibers can be distinguished. Type I fibers form few fusiform varicosities, and they establish larger terminals (boutons) close to the M-cell membrane (Fig. 3*D2*, black arrowheads). Type II fibers are thinner and form small beaded varicosities parallel to the membrane (Fig. 5*D3*, white arrowheads). Larger 5-HT-containing type I boutons terminate also onto the M-cell soma, and chains of beaded small varicosities (type II) run across the axon cap (Fig. 3*C*).

The M-cell transcriptome shows little variation. The immunohistochemical results encouraged us to examine 5-HTR expression in the M-cell at the molecular level. However, the aspiration technique we adapted to harvest the M-cell cytoplasm (see MATERIALS AND METHODS) could potentially result in a biased and highly variable representation of the mRNA pool, especially if only portions of the cytoplasm are harvested. If this were the case, we would expect a large amount of variation in gene expression across multiple M-cell samples. Therefore, we first assessed the extent of this variation by comparing the transcriptomes of three M-cells and three whole brain samples, which served as an unbiased control. After removing control features as well as those with signal intensities below threshold, we obtained data for 16,892 array features. Using a FDR-adjusted significance threshold of $P < 0.01$, we found gene expression to be differentially regulated between M-cells and whole brains for 5,026 (29.8%) of the 16,890 features, indicating the unique properties of this cell type. Specifically, 2,972 (18%) features were upregulated in M-cells and 2,054 (12%) were upregulated in whole brains.

We then examined transcriptome variation across individual samples; 16,090 features remained for this analysis after removal of control and below-threshold features. When using a significance threshold of $P < 0.01$, we found that 359 (2%) features varied significantly across M-cells, whereas 169 (1%) features were different across whole brains. However, when P values were adjusted for multiple hypotheses testing with the Benjamini-Hochberg method, there were no features that varied significantly.

Next, we used Pearson correlation analysis to quantitatively assess the extent to which transcriptomes varied across either M-cells or whole brains. We correlated the normalized intensities for all M-cell and whole brain samples, respectively, against each other and found that overall whole brains were significantly more variable (i.e., yielded smaller correlation coefficients; *t*-test, $P = 0.013$) compared with M-cells. Table 2 shows the correlation coefficients for all six pairwise comparisons.

Some 5-HT receptor subtypes are expressed in the M-cell. We cloned a single mRNA transcript each from the *A. burtoni* 5-HTR subtypes 1A, 1D, 2A, 3A/B, 5A, and 6. Subtype identities were confirmed by constructing a gene tree with the

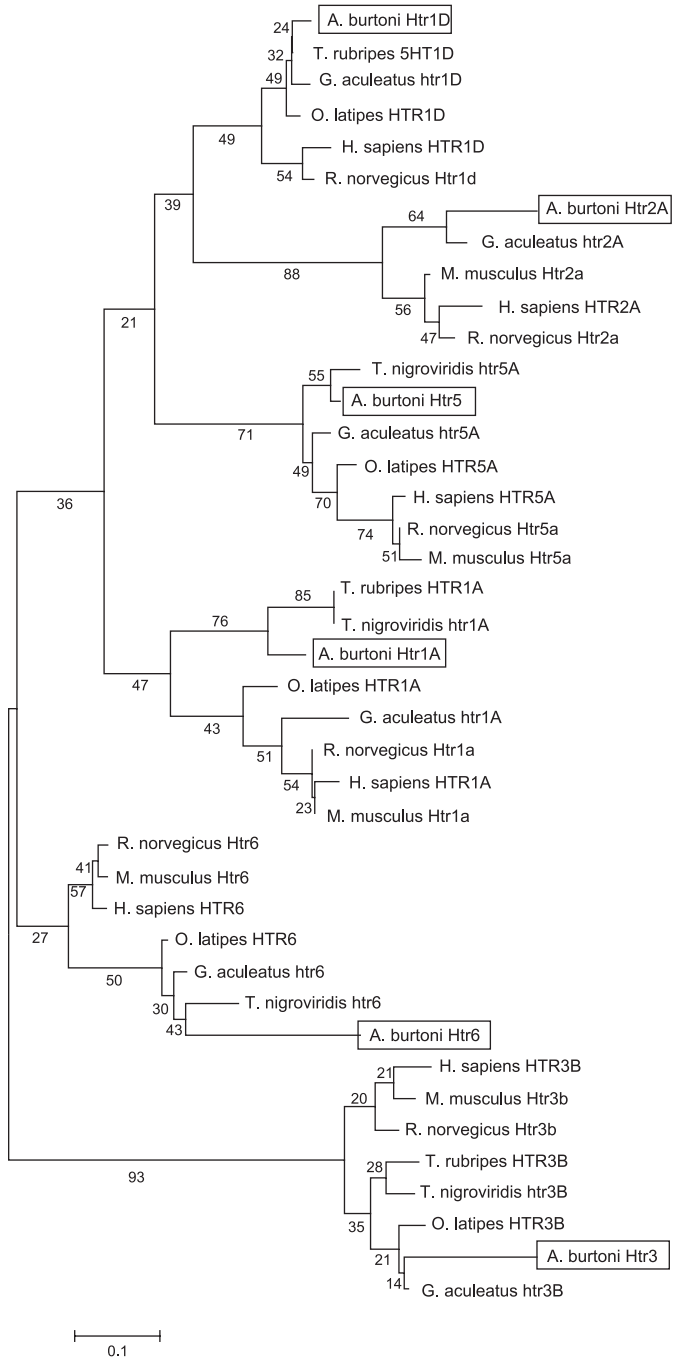

Fig. 4. Classifying 5-HTR subtypes. *Astatotilapia burtoni* 5-HTR sequences cluster with the putative 5-HTR orthologs identified in other species, confirming their subtype identities. Numbers indicate confidence values based on bootstrap analysis.

orthologous 5-HTRs of other vertebrates (Fig. 4). Next, we assessed the expression of 5-HTRs in amplified mRNA samples collected from individual M-cells ($n = 3$) and whole brains ($n = 3$) by PCR. While all receptors investigated are expressed in whole brain, only 5-HTR_{5A} and 5-HTR_6 mRNAs are present in M-cells (Fig. 5). The 5-HTR_{1A}, 5-HTR_{1D}, and 5-HTR_{3B} subtypes are clearly not present in the M-cell. Similarly, the 5-HTR_{2A} subtype is not expressed in the M-cell.

DISCUSSION

We have shown that in *A. burtoni* males both startle-escape performance and M-cell physiology are modulated by 5-HT. In particular, we found that M-cell excitability in SUBs and DOMs was differentially affected by the specific 5-HTR_2 antagonist ketanserin, suggesting a likely role of this subtype in controlling the socially regulated startle-escape plasticity observed in this species (Neumeister et al. 2010). The fact that 5-HTR_{2A} receptors are not expressed in the M-cell suggest that the observed changes in M-cell excitability (i.e., input resistance) are mediated through 5-HTR_{2A} receptors at the PHP interneurons that are part of the M-cell inhibitory system. We have further demonstrated the feasibility of obtaining high-quality and robust mRNA from single M-cells, which enabled us to reveal the 5-HTR expression pattern of the M-cell.

These results constitute a significant step forward in our understanding of social effects on neural circuits and the underlying neurochemical and molecular processes in vertebrates.

The 5-HTR_{2A} receptor subtype has been heavily studied in the context of cognition, mood disorders, and psychosis (Landolt and Wehrle 2009; Maier et al. 2008). Allee et al. (2008) were the first to employ the selective 5-HTR_2 antagonist ketanserin in another teleost, the weakly electric fish *Brachyhypopomus pinnicaudatus*, in which they demonstrated the role of this receptor subtype in modulating the electric signal waveform. To determine whether 5-HT modulates M-cell excitability via this subtype, we quantified in both DOMs and SUBs the effect of the 5-HTR_2 antagonist ketanserin on sound-evoked M-cell EPSPs in response to sound pips. Interestingly, lowering the 5-HT tone in SUBs increased the synaptic response (PSP) only if it was not already saturated by a high-intensity sound, i.e., the effect declined with increasing sound intensities. In contrast, the synaptic response in DOMs remained essentially unchanged after application of ketanserin for the entire range of sound intensities, likely indicating a ceiling effect. In a preceding study, an identical range of sound pips evoked significantly larger PSPs in DOMs compared with SUBs (Neumeister et al. 2010). The synaptic response in DOMs might thus be maximal for a given sound intensity presumably due to the already low 5-HT tone in the M-cell pre- and postsynaptic circuit and cannot be further increased by applying the 5-HTR_2 antagonist. Consistent with this notion is the fact that the amount of 5-HT and its principal metabolite in the hindbrain is lower in DOMs compared with SUBs (Winberg et al. 1997). This interpretation is further supported by the differential effects of ketanserin on the magnitude of M-cell feedback inhibition in SUBs vs. DOMs, where ketanserin affected only SUBs.

In principle, the reduction in inhibitory drive and M-cell input resistance in SUBs could be explained by both post- and presynaptic mechanisms. The two social phenotypes might differ in the degree of 5-HTR_2-mediated excitation of the inhibitory glycinergic interneurons (Koyama et al. 2011), which provide phasic and tonic inhibition to the M-cell (Faber et al. 1991; Mintz and Korn 1991). The latter hypothesis is supported by our finding that the 5-HTR_{2A} gene is not expressed in the M-cell (see below). In summary, our electrophysiological results provide strong evidence that DOMs and SUBs indeed differ at the level of M-cell physiology and underscore the utility of pharmacological approaches for uncovering the differences in the circuit mechanisms that underlie socially regulated differences in escape performance.

Our behavioral results also indicate an increase in M-cell excitability following ketanserin; however, this increase was independent of social state. How can we reconcile this discrepancy between electrophysiology and behavior? One possibility is that the injection effect described above masks any social status-specific effects. Even though *A. burtoni* males are overall quite robust when placed in a test arena (Neumeister et al. 2010) or when handled and injected with drugs (e.g., Trainor and Hofmann 2006), used in combination these methods apparently act as stressors that reduce startle responsiveness

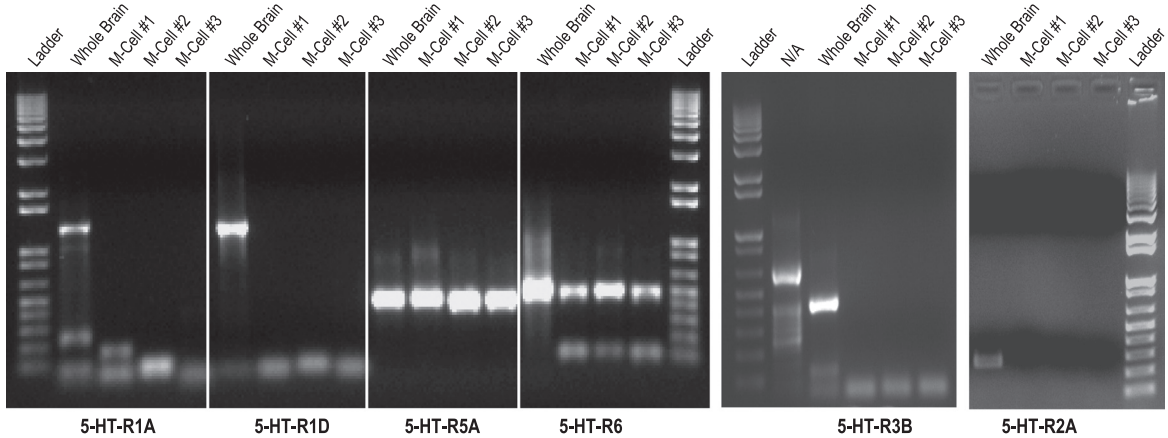

Fig. 5. Expression of 5-HTR subtypes in single M-cells. mRNAs extracted from a homogenized whole brain and 3 different M-cells were used as the template for a PCR reaction with primers specific to 5-HTR subtypes. All subtypes are present in the brain, as expected, but only subtypes 5A and 6 are present in M-cells, suggesting a postsynaptic role for 5-HT via these receptors. The subtypes 1A, 1D, 2A, and 3B are not expressed in the M-cell. N/A indicates a PCR product for a gene not examined in this study.

compared with naive animals (Neumeister et al. 2010). While this is most obvious in DOMs, SUBs also showed a decrease in responsiveness (see Fig. 1 in Neumeister et al. 2010). For the physiology experiments, on the other hand, fish were anesthetized rapidly with a high dose of anesthetic and maintained under a lower dose throughout the experiment. It is thus conceivable that these animals were less affected by stress than their counterparts in the behavioral experiments, which may explain some of the inconsistencies. In other words, the physiological measures (i.e., synaptic response and M-cell input resistance) are likely more sensitive measures for M-cell excitability than the all-or-none behavioral output. Finally, it is also possible that a more gradual onset of ketanserin applied IM during physiology experiments compared with IP in the behavior experiments could result in differential activation of the startle-escape circuit. In fact, Teshiba et al. (2001) noted that the effects of 5-HT on the lateral giant neuron of crayfish can vary depending on such pharmacokinetic processes. In summary, the observed discrepancies between the physiology and behavioral results are at least partly due to experimental constrains; however, as noted, under both conditions ketanserin increased M-cell excitability.

We found that the morphology of the paired M-cells in *A. burtoni* is comparable to the structures in goldfish (Faber and Korn 1978). In addition, 5-HT immunohistochemistry in the *A. burtoni* hindbrain indicated a distribution of 5-HT type I and II fibers similar to that of goldfish (described by Gotow et al. 1990), suggesting synaptic and paracrine modulation of the M-cell, respectively.

While these histological results were encouraging, they did not allow us to conclude which receptor subtypes, if any, might regulate M-cell function. In the absence of *A. burtoni* 5-HTR subtype-specific antibodies, we decided to examine receptor expression at the level of mRNA. Compared with the respective orthologs from other teleost species and representative mammals, our receptor sequences clearly indicated that we were successful in obtaining cDNA fragments for the genes that encode the 1A, 1D, 2A, 5A, and 6 subtypes. Because the identity of the subtype 3 sequence was more ambiguous, we have tentatively labeled it as 3B subtype. It should also be noted that because of the additional whole genome duplication event early on in teleost evolution (Meyer and Schartl 1999) additional subtypes may exist in *A. burtoni*. Since the sequencing of the *A. burtoni* genome is currently nearing completion, we will soon have the ability to identify other members of this family.

We found that the cytoplasmic aspiration technique permits a robust and reliable assessment of transcript levels in individual M-cells. Importantly, our correlation analysis showed that M-cell transcriptomes were more similar to each other than were those from whole brains, suggesting that the cytoplasmic aspiration technique does not introduce additional (technical) variation in mRNA content. Also, the correlation coefficients we obtained by comparing the transcriptomes of individual M-cells are comparable to or greater than those reported for single neurons in previous single-neuron studies (e.g., Esumi et al. 2008; Tietjen et al. 2003). There is considerable variation in gene expression throughout the brain of DOMs and SUBs (for a detailed analysis, see Renn et al. 2008). The transcriptome of M-cells is relatively stable in comparison and largely unaffected by the single-cell harvesting procedure. It should be noted that most likely we did not extract cytoplasm beyond the trunks of the major dendrites and thus might have missed mRNA species present in the dendrites, although evidence for local translation in the M-cell is currently limited to the axon (see Koenig 1979; Koenig and Martin 1996). In any case, mRNAs targeted for translocation to the periphery still need to be transcribed in the nucleus and thus would be expected to be en passant present in the cytoplasmic samples. Experiments currently underway aim to determine which 5-HTR mRNAs, if any, might be present in the dendrites.

We then analyzed the molecular substrate of M-cell physiology by assaying the expression of 5-HTRs in M-cells. Of the subtypes we have identified, only 5-HTR_{5A} and 5-HTR_6 mRNAs are present in M-cells. These results support a postsynaptic role of 5-HT in the M-cell and provide a great opportunity to learn more about the function of these receptors, given that their role in the vertebrate nervous system is still largely unclear. 5-HTR_{5A} has been associated with schizophrenia (Dubertret et al. 2004) as well as bipolar disorder and major depression (Arias et al. 2001), although its function is still only poorly understood (but see Doly et al. 2004 for its potential role in the suprachiasmatic nucleus and Sprouse et al. 2004 for nociception in the spinal cord). 5-HTR_6 has been implicated in anxiety, cognition, and the regulation of food intake (Woolley et al. 2004); however, most of the evidence is still circumstantial. Our finding that the 5-HTR_{1A} and 5-HTR_{1D} subtypes are not present in the M-cell is consistent with the notion that these subtypes play an important role as autoreceptors in serotonergic neurons (Roberts et al. 2001). We also find that the 5-HTR_{2A} and 5-HTR_{3B} subtypes are not expressed in the M-cell. This is important evidence that the effects of the 5-HTR_2 antagonist ketanserin are indeed presynaptic, likely via the inhibitory interneurons that impinge onto the M-cell, as discussed above.

5-HT is not the only neuromodulator known to affect the M-cell system. In goldfish, for example, dopamine enhances the efficacy of excitatory synapses to the M-cell LD (Pereda et al. 1992, 1994). Also in goldfish, the neuropeptide somatostatin is colocalized with glutamatergic excitatory and GABAergic inhibitory synaptic contacts that impinge onto the M-cell, an arrangement suggesting a modulatory role for this neuropeptide (Sur et al. 1994). Indeed, local application of somatostatin onto the M-cell LD increases excitatory synaptic transmission in the large club endings that provide auditory input to the cell (Pereda et al. 1997). This latter finding is interesting because somatostatin also plays an important role in regulating social behavior in *A. burtoni* (Hofmann and Fernald 2000; Trainor and Hofmann 2006, 2007).

In conclusion, the present study shows that 5-HT modulates socially regulated startle-escape responsiveness and underlying M-cell excitability, likely via presynaptic effects on inhibitory interneurons. Furthermore, we have established a powerful paradigm that will greatly facilitate the study of these and other neurochemical mechanisms at the level of behavior, electrophysiology, and single-neuron molecular biology within the same individuals.

ACKNOWLEDGMENTS

We thank Dr. Michael Markham for advice on the ketanserin experiments, Dr. Steve Walkley and colleagues for help with the immunohistochemistry, and Marcos Alvarez for technical assistance. Dr. Donald Faber loaned a high-speed camera, and Dr. Harold Zakon provided generous access to his

laboratory. We also thank Dr. Michael Markham and Leslie Whitaker for critically reading earlier versions of this manuscript and members of the Hofmann and Preuss laboratories for discussions.

GRANTS

This work was supported by the Department of Defense SMART program (K. W. Whitaker); National Science Foundation (NSF)-IOS Grant 0946637, Hunter College of CUNY, and Research Foundation of CUNY (T. Preuss); and NSF-IOS Grant 0751311, the Alfred P. Sloan Foundation, and the Institute for Cellular and Molecular Biology at the University of Texas at Austin (H. A. Hofmann).

DISCLOSURES

No conflicts of interest, financial or otherwise, are declared by the author(s).

REFERENCES

Allee SJ, Markham MR, Salazar VL, Stoddard PK. Opposing actions of 5HT1A and 5HT2-like serotonin receptors on modulations of the electric signal waveform in the electric fish *Brachyhypopomus pinnicaudatus*. *Horm Behav* 53: 481–488, 2008.

Antonsen BL, Edwards DH. Mechanisms of serotonergic facilitation of a command neuron. *J Neurophysiol* 98: 3494–3504, 2007.

Arias B, Collier DA, Gastó C, Pintor L, Gutiérrez B, Vallès V, Fañanás L. Genetic variation in the 5-HT5A receptor gene in patients with bipolar disorder and major depression. *Neurosci Lett* 303: 111–114, 2001.

Baugh LR, Hill AA, Brown EL, Hunter CP. Quantitative analysis of mRNA amplification by in vitro transcription. *Nucleic Acids Res* 29: E29, 2001.

Benjamini Y, Hochberg Y. On the adaptive control of the false discovery rate in multiple testing with independent statistics. *J Educ Behav Stat* 25: 60–83, 2000.

Bierman HS, Zottoli SJ, Hale ME. Evolution of the Mauthner axon cap. *Brain Behav Evol* 73: 174–187, 2009.

Brustein E, Chong M, Holmqvist B, Drapeau P. Serotonin patterns locomotor network activity in the developing zebrafish by modulating quiescent periods. *J Neurobiol* 57: 303–322, 2003.

Canfield JG. Temporal constraints on visually directed C-start responses: behavioral and physiological correlates. *Brain Behav Evol* 61: 148–158, 2003.

Canfield JG, Rose GJ. Hierarchical sensory guidance of Mauthner-mediated escape responses in goldfish (*Carassius auratus*) and cichlids (*Haplochromis burtoni*). *Brain Behav Evol* 48: 137–156, 1996.

Churchill GA. Fundamentals of experimental design for cDNA microarrays. *Nat Genet* 32: 490–495, 2002.

Crews D. The development of phenotypic plasticity: where biology and psychology meet. *Dev Psychobiol* 43: 1–10, 2003.

Deco G, Rolls ET. Attention, short-term memory, and action selection: a unifying theory. *Prog Neurobiol* 76: 236–256, 2005.

Dickson BJ. Wired for sex: the neurobiology of *Drosophila* mating decisions. *Science* 322: 904–909, 2008.

Doly S, Fischer J, Brisorgueil MJ, Vergé D, Conrath M. 5-HT5A receptor localization in the rat spinal cord suggests a role in nociception and control of pelvic floor musculature. *J Comp Neurol* 476: 316–329, 2004.

Dubertret C, Hanoun N, Adès J, Hamon M, Gorwood P. Family-based association studies between 5-HT5A receptor gene and schizophrenia. *J Psychiatr Res* 38: 371–376, 2004.

Duftner N, Larkins-Ford J, Legendre M, Hofmann HA. Efficacy of RNA amplification is dependent on sequence characteristics: implications for gene expression profiling using a cDNA microarray. *Genomics* 91: 108–117, 2008.

Eaton RC, DiDomenico R, Nissanov J. Role of the Mauthner cell in sensorimotor integration by the brain stem escape network. *Brain Behav Evol* 37: 272–285, 1991.

Eberwine J. Single-cell molecular biology. *Nat Neurosci* 4 Suppl: 1155–1156, 2001.

Edwards DH, Kravitz EA. Serotonin, social status and aggression. *Curr Opin Neurobiol* 7: 812–819, 1997.

Edwards DH, Yeh SR, Musolf BE, Antonsen BL, Krasne FB. Metamodulation of the crayfish escape circuit. *Brain Behav Evol* 60: 360–369, 2002.

Edwards DH, Heitler WJ, Krasne FB. Fifty years of a command neuron: the neurobiology of escape behavior in the crayfish. *Trends Neurosci* 22: 153–161, 1999.

Edwards DH, Issa FA, Herberholz J. The neural basis of dominance hierarchy formation in crayfish. *Microsc Res Tech* 60: 369–376, 2003.

Esumi S, Wu SX, Yanagawa Y, Obata K, Sugimoto Y, Tamamaki N. Method for single-cell microarray analysis and application to gene-expression profiling of GABAergic neuron progenitors. *Neurosci Res* 60: 439–451, 2008.

Faber DS, Korn H. *Neurobiology of the Mauthner Cell*. New York: Raven, 1978.

Faber DS, Korn H, Lin JW. Role of medullary networks and postsynaptic membrane properties in regulating Mauthner cell responsiveness to sensory excitation. *Brain Behav Evol* 37: 286–297, 1991.

Feder A, Nestler EJ, Charney DS. Psychobiology and molecular genetics of resilience. *Nat Rev Neurosci* 10: 446–457, 2009.

Fernald RD. Social regulation of the brain: sex, size and status. *Novartis Found Symp* 244: 169–184, 2002.

Fernald RD, Hirata NR. Field study of *Haplochromis burtoni*: habitats and co-habitants. *Environ Biol Fishes* 2: 299–308, 1977.

Flores CE, Ene S, Pereda AE. An immunochemical marker for goldfish Mauthner cells. *J Neurosci Methods* 175: 64–69, 2008.

Furukawa T, Furshpan EJ. Two inhibitory mechanisms in the Mauthner neurons of goldfish. *J Neurophysiol* 26: 140–176, 1963.

Goodson JL, Evans AK, Soma KK. Neural responses to aggressive challenge correlate with behavior in nonbreeding sparrows. *Neuroreport* 16: 1719–1723, 2005.

Gotow T, Triller A, Korn H. Differential distribution of serotonergic inputs on the goldfish Mauthner cell. *J Comp Neurol* 299: 255–268, 1990.

Hinkle D, Glanzer J, Sarabi A, Pajunen T, Zielinski J, Belt B, Miyashiro K, McIntosh T, Eberwine J. Single neurons as experimental systems in molecular biology. *Prog Neurobiol* 72: 129–142, 2004.

Hofmann HA. Functional genomics of neural and behavioral plasticity. *J Neurobiol* 54: 272–282, 2003.

Hofmann HA, Fernald RD. Social status controls somatostatin neuron size and growth. *J Neurosci* 20: 4740–4744, 2000.

Imboden M, Devignot V, Korn H, Goblet C. Regional distribution of glycine receptor messenger RNA in the central nervous system of zebrafish. *Neuroscience* 103: 811–830, 2001.

Koenig E. Ribosomal RNA in Mauthner axon: implications for a protein synthesizing machinery in the myelinated axon. *Brain Res* 174: 95–107, 1979.

Koenig E, Martin R. Cortical plaque-like structures identify ribosome-containing domains in the Mauthner cell axon. *J Neurosci* 16: 1400–1411, 1996.

Kohno K, Noguchi N. Large myelinated club endings on the Mauthner cell in the goldfish: a study with thin sectioning and freeze-fracturing. *Anat Embryol (Berl)* 173: 361–370, 1986.

Korn H, Faber DS. The Mauthner cell half a century later: a neurobiological model for decision-making? *Neuron* 47: 13–28, 2005.

Koyama M, Kinkhabwala A, Satou C, Higachijima S, Fetcho J. Mapping a sensory-motor network onto a structural and functional ground plan in the hindbrain. *Proc Natl Acad Sci USA* 108: 1170–1175, 2011.

Krasne FB, Shamsian A, Kulkarni R. Altered excitability of the crayfish lateral giant escape reflex during agonistic encounters. *J Neurosci* 17: 709–716, 1997.

Krishnan V, Nestler EJ. The molecular neurobiology of depression. *Nature* 455: 894–902, 2008.

Kurimoto K, Saitou M. Single-cell cDNA microarray profiling of complex biological processes of differentiation. *Curr Opin Genet Dev* 20: 470–477, 2010.

Landolt HP, Wehrle R. Antagonism of serotonergic 5-HT2A/2C receptors: mutual improvement of sleep, cognition and mood? *Eur J Neurosci* 29: 1795–1809, 2009.

Maan ME, Eshuis B, Haesler MP, Schneider MV, van Alphen JJM, Seehausen O. Color polymorphism and predation in a Lake Victoria cichlid fish. *Copeia* 3: 621–629, 2008.

Maier W, Mössner R, Quednow BB, Wagner M, Hurlemann R. From genes to psychoses and back: the role of the 5HT2alpha-receptor and prepulse inhibition in schizophrenia. *Eur Arch Psychiatry Clin Neurosci* 258, *Suppl* 5: 40–43, 2008.

Martin KC. Local protein synthesis during axon guidance and synaptic plasticity. *Curr Opin Neurobiol* 14: 305–310, 2004.

McClung CA, Nestler EJ. Neuroplasticity mediated by altered gene expression. *Neuropsychopharmacology* 33: 3–17, 2008.

McLean DL, Fetcho JR. Relationship of tyrosine hydroxylase and serotonin immunoreactivity to sensorimotor circuitry in larval zebrafish. *J Comp Neurol* 29: 57–71, 2004.

Meyer A, Schartl M. Gene and genome duplications in vertebrates: the one-to-four (-to-eight in fish) rule and the evolution of novel gene functions. *Curr Opin Cell Biol* 11: 699–704, 1999.

Mintz I, Korn H. Serotonergic facilitation of quantal release at central inhibitory synapses. *J Neurosci* 11: 3359–3370, 1991.

Mintz I, Gotow T, Triller A, Korn H. Effect of serotonergic afferents on quantal release at central inhibitory synapses. *Science* 245: 190–200, 1989.

Munro AD. Effects of melatonin, serotonin, and naloxone on aggression in isolated cichlid fish, *Aequidens pulcher*. *J Pineal Res* 3: 257–262, 1986.

Neumeister H, Szabo TM, Preuss T. Behavioral and physiological characterization of sensorimotor gating in the goldfish startle response. *J Neurophysiol* 99: 1493–1502, 2008.

Neumeister HK, Whitaker KW, Hofmann HA, Preuss T. Social and ecological regulation of a decision-making circuit. *J Neurophysiol* 104: 3180–3188, 2010.

Newman SW. The medial extended amygdala in male reproductive behavior. A node in the mammalian social behavior network. *Ann NY Acad Sci* 877: 242–257, 1999.

O'Connell LA, Hofmann HA. Genes, hormones, and circuits: an integrative approach to study the evolution of social behavior. *Front Neuroendocrinol* (December 14, 2010). doi: 10.1016/j.yfrne.2010.12.004.

O'Connell LA, Hofmann HA. The vertebrate mesolimbic reward system and social behavior network: a comparative synthesis. *J Comp Neurol*. In press.

Pereda A, O'Brien J, Nagy JI, Bukauskas F, Davidson KG, Kamasawa N, Yasumura T, Rash JE. Connexin35 mediates electrical transmission at mixed synapses on Mauthner cells. *J Neurosci* 23: 7489–7503, 2003.

Pereda AE, Nairn AC, Wolszon LR, Faber DS. Postsynaptic modulation of synaptic efficacy at mixed synapses on the Mauthner cell. *J Neurosci* 14: 3704–3712, 1994.

Pereda A, Reisine T, Faber DS, Korn H. Somatostatin enhances excitatory synaptic transmission at mixed synapses on the Mauthner (M-) cell. *Neurosci Soc Abstr* 23: 1180, 1997.

Pereda A, Triller A, Korn H, Faber DS. Dopamine enhances both electrotonic coupling and chemical excitatory postsynaptic potentials at mixed synapses. *Proc Natl Acad Sci USA* 89: 12088–12092, 1992.

Petrov T, Seitanidou T, Triller A, Korn H. Differential distribution of GABA- and serotonin-containing afferents on an identified central neuron. *Brain Res* 559: 75–81, 1991.

Preuss T, Faber DS. Central cellular mechanisms underlying temperature-dependent changes in the goldfish startle-escape behavior. *J Neurosci* 23: 5617–5626, 2003.

Preuss T, Osei-Bonsu PE, Weiss SA, Wang C, Faber DS. Neural representation of object approach in a decision-making motor circuit. *J Neurosci* 26: 3454–3464, 2006.

Renn SC, Aubin-Horth N, Hofmann HA. Biologically meaningful expression profiling across species using heterologous hybridization to a cDNA microarray. *BMC Genomics* 5: 42, 2004.

Renn SC, Aubin-Horth N, Hofmann HA. Fish and chips: functional genomics of social plasticity in an African cichlid fish. *J Exp Biol* 211: 3041–3056, 2008.

Roberts C, Price GW, Middlemiss DN. Ligands for the investigation of 5-HT autoreceptor function. *Brain Res Bull* 56: 463–469, 2001.

Robinson GE, Fernald RD, Clayton DF. Genes and social behavior. *Science* 322: 896–900, 2008.

Salzburger W, Renn SC, Steinke D, Braasch I, Hofmann HA, Meyer A. Annotation of expressed sequence tags for the East African cichlid fish *Astatotilapia burtoni* and evolutionary analyses of cichlid ORFs. *BMC Genomics* 9: 96, 2008.

Satou C, Kimura Y, Kohashi T, Horikawa K, Takeda H, Oda Y, Higashijima S. Functional role of a specialized class of spinal commissural inhibitory neurons during fast escapes in zebrafish. *J Neurosci* 29: 6780–6793, 2009.

Schlegel T, Schuster S. Small circuits for large tasks: high-speed decision-making in archerfish. *Science* 319: 104–106, 2008.

Smyth GK. Limma: linear models for microarray data. In: *Bioinformatics and Computational Biology Solutions Using R and Bioconductor*, edited by Gentleman R, Carey V, Dudoit S, Irizarry R, Huber W. New York: Springer, 2005, p. 397–420.

Smyth GK, Thorne NP, Wettenhall J. *LIMMA: Linear Models for Microarray Data, Version 1.6.6, User's Guide*. 2004 [http://bioinf.wehi.edu.au/limma/].

Sotelo-Silveira JR, Calliari A, Cárdenas M, Koenig E, Sotelo JR. Myosin Va and kinesin II motor proteins are concentrated in ribosomal domains (periaxoplasmic ribosomal plaques) of myelinated axons. *J Neurobiol* 60: 187–196, 2004.

Spitzer N, Antonsen BL, Edwards DH. Immunocytochemical mapping and quantification of expression of a putative type 1 serotonin receptor in the crayfish nervous system. *J Comp Neurol* 484: 261–282, 2005.

Sprouse J, Reynolds L, Braselton J, Schmidt A. Serotonin-induced phase advances of SCN neuronal firing in vitro: a possible role for 5-HT5A receptors? *Synapse* 54: 111–118, 2004.

Sur C, Korn H, Triller A. Colocalization of somatostatin with GABA or glutamate in distinct afferent terminals presynaptic to the Mauthner cell. *J Neurosci* 14: 576–589, 1994.

Szabo TM, Brookings T, Preuss T, Faber DS. Effects of temperature acclimation on a central neural circuit and its behavioral output. *J Neurophysiol* 100: 2997–3008, 2008.

Teshiba T, Shamsian A, Yashar B, Yeh SR, Edwards DH, Krasne FB. Dual and opposing modulatory effects of serotonin on crayfish lateral giant escape command neurons. *J Neurosci* 21: 4523–4529, 2001.

Tietjen I, Rihel JM, Cao Y, Koentges G, Zakhary L, Dulac C. Single-cell transcriptional analysis of neuronal progenitors. *Neuron* 24: 161–175, 2003.

Trainor BC, Hofmann HA. Somatostatin and somatostatin receptor gene expression in dominant and subordinate males of an African cichlid fish. *Behav Brain Res* 179: 314–320, 2007.

Trainor BC, Hofmann HA. Somatostatin regulates aggressive behavior in an African cichlid fish. *Endocrinology* 147: 5119–5125, 2006.

Triller A, Nicola MA, Coudrier E, Louvard D, Korn H. A monoclonal antibody raised against the Mauthner cell also recognizes some reticular neurons. *Neuroscience* 41: 277–285, 1991.

Turner GF, Pitcher TJ. Attack abatement: a model for group protection by combined avoidance and dilution. *Am Nat* 128: 228–240, 1986.

Veenema AH. Early life stress, the development of aggression and neuroendocrine and neurobiological correlates: what can we learn from animal models? *Front Neuroendocrinol* 30: 497–518, 2009.

Weiss SA, Preuss T, Faber DS. A role of electrical inhibition in sensorimotor integration. *Proc Natl Acad Sci USA* 105: 18047–18052, 2008.

Weiss SA, Zottoli SJ, Do SC, Faber DS, Preuss T. Correlation of C-start behaviors with neural activity recorded from the hindbrain in free-swimming goldfish (*Carassius auratus*). *J Exp Biol* 209: 4788–4801, 2006.

Winberg S, Winberg Y, Fernald RD. Effect of social rank on brain monoaminergic activity in a cichlid fish. *Brain Behav Evol* 49: 230–236, 1997.

Wong RY, Hofmann HA. Behavioral genomics: an organismal perspective. In: *Encyclopedia of Life Sciences*. Chichester, UK: Wiley, 2010.

Woolley ML, Marsden CA, Fone KC. 5-ht6 receptors. *Curr Drug Targets CNS Neurol Disord* 3: 59–79, 2004.

Yeh SR, Fricke RA, Edwards DH. The effect of social experience on serotonergic modulation of the escape circuit of crayfish. *Science* 271: 366–369, 1996.

Yeh SR, Musolf BE, Edwards DH. Neuronal adaptations to changes in the social dominance status of crayfish. *J Neurosci* 17: 697–708, 1997.